

Article

On the Theory of Unsteady-State Operation of Bulk Continuous Crystallization

Eugenia V. Makoveeva ^{1,2,*}, Dmitri V. Alexandrov ^{1,2}  and Alexander A. Ivanov ² 

¹ Laboratory of Stochastic Transport of Nanoparticles in Living Systems, Ural Federal University, Lenin Ave., 51, Ekaterinburg 620000, Russia

² Laboratory of Multi-Scale Mathematical Modeling, Department of Theoretical and Mathematical Physics, Ural Federal University, Lenin Ave., 51, Ekaterinburg 620000, Russia

* Correspondence: e.v.makoveeva@urfu.ru

Abstract: Motivated by an important application in the chemical and pharmaceutical industries, we consider the non-stationary growth of a polydisperse ensemble of crystals in a continuous crystallizer. The mathematical model includes the effects of crystal nucleation and growth, fines dissolution, mass influx and withdrawal of product crystals. The steady- and unsteady-state solutions of kinetic and balance equations are analytically derived. The steady-state solution is found in an explicit form and describes the stationary operation mode maintained by the aforementioned effects. An approximate unsteady-state solution is found in a parametric form and describes a time-dependent crystallization scenario, which tends toward the steady-state mode when time increases. It is shown that the particle-size distribution contains kinks at the points of fines dissolution and product crystal withdrawal. Additionally, our calculations demonstrate that the unsteady-state crystal-size distribution has a bell-shaped profile that blurs with time due to the crystal growth and removal mechanisms. The analytical solutions found are the basis for investigating the dynamic stability of a continuous crystallizer.

Keywords: crystal growth; nucleation; evolution of particulate assemblages; mathematical modeling; analytical solutions



Citation: Makoveeva, E.V.; Alexandrov, D.V.; Ivanov, A.A. On the Theory of Unsteady-State Operation of Bulk Continuous Crystallization. *Crystals* **2022**, *12*, 1634. <https://doi.org/10.3390/cryst12111634>

Academic Editor: Pavel Lukáč

Received: 28 October 2022

Accepted: 11 November 2022

Published: 14 November 2022

Publisher's Note: MDPI stays neutral with regard to jurisdictional claims in published maps and institutional affiliations.



Copyright: © 2022 by the authors. Licensee MDPI, Basel, Switzerland. This article is an open access article distributed under the terms and conditions of the Creative Commons Attribution (CC BY) license (<https://creativecommons.org/licenses/by/4.0/>).

1. Introduction

Volumetric and directional crystallization processes are the basis for many technological processes for growing crystals with certain physical and chemical properties [1–5]. As a rule, in highly supersaturated solutions and supercooled melts, nucleation occurs on microscopic inclusions that are always present in the liquid phase (e.g., particles of dissolved impurity, dust or foreign microparticles present in the liquid). Then, if the size of the formed particles of the solid phase exceeds the critical size, the crystallites are viable and capable of growth. If the size of the formed particles is smaller than the critical size, such particles dissolve. The more the system is supersaturated (supercooled), the more viable crystals will be present, and the greater the nucleation rate (frequency). As a rule, this important feature of a metastable system is described by means of the experimentally well-founded Meirs law for nucleation kinetics or the theoretical the Weber–Volmer–Frenkel–Zel'dovich (WVfZ) kinetics law [6–8]. In addition to the nucleation kinetics, the bulk-phase-transformation process is significantly influenced by a number of other factors. These include, for example, the crystal growth rate law (quasi-stationary, non-stationary, empirical) [9–14]; the shape hypothesis of growing crystals (spherical and ellipsoidal or irregular shape approximations) [15–20]; external mass inflows or heat dissipation through system boundaries [21–25]; the type and shape of the crystallizer [26,27]; the presence or absence of stirring in the bath liquid [28,29], crystal discharge from the crystallizer [30,31]; the presence or absence of crystal fragmentation, attrition, coagulation and Ostwald ripening processes [32–38]; simultaneous occurrence of nucleation and directional solidification [39,40]; and other factors. Simultaneous consideration of all these characteristics in a single mathematical model of

the crystallizer is hardly possible due to its extreme complexity. Therefore, one way is to take into account in the model the most important factors for a particular type of process under study. For example, an analytical theory with an allowance for the heat exchange of a supercooled liquid with the environment while there is a constant withdrawal rate of product crystals was constructed in references [24,30]. In addition, the influence of the polymerization process on the operation of an ideal mixing crystallizer was investigated in references [31,41], whereas the process of formation of self-oscillatory crystallizer operation mode was investigated with the help of stability theory in references [21,42–44].

In the present work, an analytical theory is constructed which takes into account simultaneously such processes as (i) nucleation and growth of crystals, (ii) their dissolution, (iii) influx of impurity into the supersaturated liquid of the crystallizer and (iv) withdrawal of product crystals from the supersaturated solution. The paper is organized as follows. In Section 2, a mathematical model of the process is formulated and its analytical solution is constructed. Also, in Section 2, an analysis of these solutions is performed. The main conclusions are given in Section 3.

2. The Integro-Differential Model and Its Analytical Solution

Let us first formulate the mathematical model of the continuous operation of an isothermal crystallizer with ideal mixing using the following physical assumptions: (i) the critical radius of nucleating crystals that are capable of further growth is negligible; (ii) the growth rate does not depend on the size of a crystal (kinetic mode); and (iii) there is no crystal fragmentation, attrition, coagulation or Ostwald ripening. A scheme of a crystallizer is shown in Figure 1. The working principle of this crystallizer is as follows [22]. A liquid solution is supplied to the working chamber of the crystallizer. Its supersaturated state is achieved through the cooling of the working chamber. Supersaturation of the solution creates conditions for nucleation and growth of crystals. The product crystals that have grown to a certain size are removed from the crystallizer.

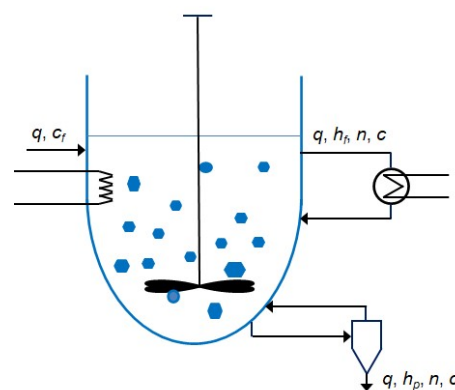


Figure 1. A scheme of continuous crystallizer with ideal mixing, isothermal operation and constant overall volume (liquid phase and growing crystals). The classification functions $h_f(r) = R_1(1 - h(r - r_f))$ and $h_p(r) = 1 + R_2h(r - r_p)$ that, respectively, define the size-dependence of fines dissolution and product withdrawal, are considered to be piecewise-constant.

Assuming that the growing crystals are spherical, let us write the kinetic equation for the particle-radius distribution function $n(r, t)$:

$$\frac{\partial n}{\partial t} = -G(c) \frac{\partial n}{\partial r} - \frac{q}{V} f(r) n(r, t), \quad (1)$$

where r and t represent the radial and time variables; $G(c) = k_g[c(t) - c_s]^g$ is the concentration-dependent growth rate of crystals; $c(t)$ and c_s are the current concentration in the working chamber and concentration at saturation; q is the feed rate; V is the total volume; and k_g and g are the growth rate constant and growth rate exponent. Generally speaking, the

classification function $f(r)$ can be chosen in various ways. Following the paper [22], let us consider the simple case where withdrawal of product crystals and dissolution of fines occur at the same rate q . Taking this into account, we chose $f(r)$ as follows [22]:

$$f(r) = R_1(1 - h(r - r_f)) + 1 + R_2h(r - r_p), \quad (2)$$

where $h(r)$ stands for the Heaviside step function, r_f is the fines-removal cut size and r_p is the product-class cut size. By paying attention to Equation (2), we can see that crystals dissolve at $r < r_f$ with the fines-removal constant R_1 and do not dissolve at $r \geq r_f$. In addition, if crystal size exceeds r_p ($r \geq r_p$), such a product crystal is removed with the withdrawal constant R_2 , and the crystal is returned to the system if $r < r_p$.

Equation (1) should be supplemented by the initial and boundary conditions [22]

$$n(r, 0) = n_0(r), \quad n(0, t) = \frac{B(c)}{G(c)}, \quad (3)$$

where $B(c) = k_b(c(t) - c_s)^b$ is the nucleation rate, and k_b and b are the nucleation rate constant and nucleation-rate exponent.

The solute mass balance equation reads as [22]

$$M \frac{dc}{dt} = \frac{q(\rho - Mc)}{V} + \frac{\rho - Mc}{\varepsilon} \frac{d\varepsilon}{dt} + \frac{qMc_f}{V\varepsilon} - \frac{q\rho}{V\varepsilon} \left(1 + k_v R_2 \int_0^\infty h(r - r_p) n(r, t) r^3 dr \right), \quad (4)$$

where ρ is the crystal density, M is the molar mass of crystals, c_f is the feed concentration, k_v is the volumetric shape factor and ε is the void fraction.

$$\varepsilon = \frac{V_{\text{liquid}}}{V} = 1 - \frac{V_{\text{solid}}}{V} = 1 - k_v \int_0^\infty n(r, t) r^3 dr.$$

In addition, the initial concentration should be regarded as known; i.e., $c(0) = c_0$. Note that the last term in Equation (4) expresses the mass outflux due to the growth and withdrawal of crystals.

Model (1)–(4) is a closed system and describes the evolution of the crystal system in the supersaturated liquid of the crystalliser, taking into account the physical hypotheses made above. Let us especially note that the model takes the initial state into account only by means of an initial distribution function (first expression (3)) and known initial concentration c_0 , although, at a very beginning, new aggregates of solid phase are formed by the nucleation process. This is due to the fact that our model describes the process of crystal-ensemble evolution in the crystallizer on macroscopic scales exceeding tens of seconds in order of magnitude (see the more detailed explanation of characteristic crystallization size and time scales at the end of this section).

Note that the model under consideration does not take into account the influence of surface energy on the evolution of crystal ensemble. This, in particular, is caused by considering an intermediate stage of phase transitions when particles (crystals) are located far enough from each other and interactions between them can be neglected. On the other hand, the surface tension leads to a shift in the phase transition temperature of each crystal due to the Gibbs–Thomson effect [45]. This in turn changes the crystal growth rate $G(c)$. However, since our theory uses the empirical power law for $G(c)$, the surface energy is not explicitly present in the model.

2.1. The Steady-State Solutions

Now, assuming that nothing depends on time t , we integrate Equation (1), keeping in mind the boundary condition (3). The steady-state particle-radius distribution function $n_{ss}(r)$ has the form

$$n_{ss}(r) = \begin{cases} c_0 \exp\left(-\frac{q(1+R_1)r}{VG(c_{ss})}\right), & 0 < r \leq r_f, \\ c_0 \exp\left(-\frac{q(r+R_1r_f)}{VG(c_{ss})}\right), & r_f < r < r_p, \\ c_0 \exp\left(-\frac{q[(1+R_2)r+R_1r_f-R_2r_p]}{VG(c_{ss})}\right), & r_p \leq r, \end{cases} \quad (5)$$

where the constant c_0 is given by

$$c_0 = \frac{B(c_{ss})}{G(c_{ss})} = \frac{\Lambda k_b}{k_g}, \quad \Lambda = \frac{(c_{ss} - c_s)^b}{(c_{ss} - c_s)^g}.$$

The steady-state solute concentration c_{ss} is defined by the solute mass balance (4) and satisfies the integral equation

$$Mc_{ss}\varepsilon_{ss} - Mc_f + \rho k_v I_c = 0, \quad (6)$$

where

$$I_c = \int_0^{\infty} [1 + R_2 h(r - r_p)] n_{ss}(r) r^3 dr, \quad \varepsilon_{ss} = 1 - k_v \int_0^{\infty} n_{ss}(r) r^3 dr.$$

Figure 2 illustrates the steady-state distribution function with different values of the nucleation and growth rate constants. Due to the fines dissolution (at $r < r_f$) and the withdrawal of product crystals (at $r > r_p$), the particle distributions have kinks at points $r = r_f$ and $r = r_p$. As this takes place, the more intense the crystal nucleation (more b), the higher in value the corresponding distribution function. As the crystal growth rate increases (higher values of g), the particles reach size r_p faster and withdraw from the system.

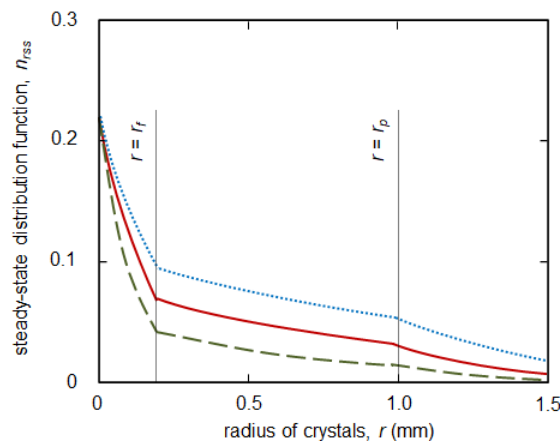


Figure 2. The steady-state particle-radius distribution $n_{r_{ss}} = n_{ss}/\Lambda$ for different nucleation and growth rate constants: $b = g = 1$ (solid line); $b = 1, g = 1.5$ (dashed line); $b = 1.5, g = 1$ (dotted line). Parameter values for a laboratory-scale KCl crystallizer are [22]: $r_f = 0.2$ mm, $r_p = 1$ mm, $R_1 = 5$, $R_2 = 2$, $q = 0.05$ L/min, $V = 10.5$ L, $k_b = 2.05 \cdot 10^{-2}$ L³/(min mol⁴), $k_g = 9.15 \cdot 10^{-2}$ mm L/(min mol), $\rho = 1989$ gr/L, $M = 74.551$ gr/mol, $k_v = 0.1112$, $c_s = 4.038$ mol/L and $c_{ss} = 4.091$ mol/L for the solid line.

2.2. The Unsteady-State Solutions

To find the unsteady-state solution, we introduce the modified time x and the natural logarithm of the distribution function N as follows.

$$t(x) = \int_0^x \frac{dx_1}{G(c(x_1))}, \quad N(r, x) = \ln n(r, t). \quad (7)$$

By rewriting (1) and (3) and using (7), we get

$$\begin{aligned} \frac{\partial N}{\partial x} + \frac{\partial N}{\partial r} + \frac{q}{V} \frac{f(r)}{G(c(x))} &= 0, \\ N(r, 0) = \ln n_0(r), \quad N(0, x) &= \ln Q(c(x)), \end{aligned} \quad (8)$$

where $Q(c(x)) = B(c(x))/G(c(x))$. The boundary-value problem (8) can be solved using the Laplace integral transform with respect to r as follows:

$$N^*(s, x) = \int_0^\infty \exp(-sr)N(r, x)dr. \quad (9)$$

Now, by rewriting (8) by means of (9) in the Laplace transform image space, we obtain

$$\begin{aligned} sN^* + \frac{dN^*}{dx} &= \ln Q(c(x)) - \frac{q}{V} f^* R(c(x)), \\ N^* &= (\ln n_0(r))^*, \quad x = 0, \end{aligned} \quad (10)$$

where $R(c(x)) = 1/G(c(x))$. Here, s represents the Laplace transform variable and superscript $*$ denotes the Laplace transform image space.

Integration of Equation (10) gives

$$\begin{aligned} N^*(s, x) &= (\ln n_0(r))^* \exp(-sx) + \int_0^x \exp(-s(x-x_1)) \ln Q(c(x_1)) dx_1 \\ &\quad - \frac{q}{V} \int_0^x \exp(-s(x-x_1)) f^* R(c(x_1)) dx_1. \end{aligned} \quad (11)$$

While taking the inverse Laplace transforms ($\delta(x)$ is the Dirac delta function) [46,47]

$$\exp(-as)g^*(s) \rightarrow \begin{cases} g(x-a), & x > a \geq 0 \\ 0, & x < a \end{cases}, \quad \exp(-as) \rightarrow \delta(x-a)$$

into account, we arrive at the distribution function

$$n(r, x) = \begin{cases} n_0(r-x)Q[c(r-x)] \exp \left[-\frac{q}{V} \int_0^x F(x_1)R(c(x_1))dx_1 \right], & r > x \\ Q[c(x-r)] \exp \left[-\frac{q}{V} \int_0^x F(x_1)R(c(x_1))dx_1 \right], & r < x \end{cases}, \quad (12)$$

where

$$F(r, r_1, x) = \begin{cases} f(r - (x - x_1)), & r > x - x_1 \geq 0 \\ 0, & r < x - x_1 \end{cases}$$

and the initial distribution function $n_0(0)$ is normalized to unity. In this case, expression (12) is continuous at $r = x$.

Thus, the exact analytical solution (12) defines the particle-radius distribution function dependent on solute concentration, c . To plot $n(r, x)$, let us develop below the following approximate method. First of all, we consider here the case of insignificant changes in the solute concentration (according to reference [22], the fluctuations in concentration are a few tenths of a percent). In this case, to obtain a good (main) approximation of the particle-radius distribution function $n(r, x) = n_m(r, x)$, one can change $c(x)$ in (12) to a constant solute concentration (e.g., by the initial or steady-state value c_{ss} , which can be set in the working chamber of the crystallizer at the initial start-up of its operation).

Keeping this in mind, the main contribution of the distribution function reads as

$$n(r, x) = n_0(r, x) = \begin{cases} n_0(r - x) Q(c_{ss}) \exp \left[-\frac{qR(c_{ss})}{V} \int_0^x F(x_1) dx_1 \right], & r > x \\ Q(c_{ss}) \exp \left[-\frac{qR(c_{ss})}{V} \int_0^x F(x_1) dx_1 \right], & r < x \end{cases} \quad (13)$$

By substituting (13) into (4) and rewriting it in terms of the modified time variable x , we come to

$$M \frac{dc}{dx} G(c(x)) = \frac{q(\rho - Mc)}{V} + \frac{\rho - Mc}{\varepsilon(x)} \frac{d\varepsilon}{dx} G(c(x)) + \frac{qMc_f}{V\varepsilon(x)} - \frac{q\rho}{V\varepsilon(x)} \left(1 + k_v R_2 \int_0^\infty h(r - r_p) n(r, t) r^3 dr \right), \quad \varepsilon(x) = 1 - k_v \int_0^\infty n(r, x) r^3 dr. \quad (14)$$

Now, taking the initial condition $c(0) = c_0$ into account, we have the Cauchy problem for the determination of main approximation $c(x) = c_m(x)$ for solute concentration (at $n = n_m$ in Equation (14)). A more accurate approximation $n(r, x) = n_1(r, x)$ to the distribution function (13) can be found by substitution of $c_m(x)$ from (14) into (12). In turn, by substituting this better approximation $n_1(r, x)$ into the Cauchy problem (14), we can find a more precise approximation for $c(x) = c_1(x)$. As this takes place, Equation (7) determines the real time as a function of modified time x . In other words, the solution is found in a parametric form with x being the decision variable.

These solutions are shown in Figure 3. Here we see that the particle-size distributions (curves marked by symbols for various x) approach the steady-state profile (solid line) when time t and modified time x increase. This means that the solutions shown in Figure 3 are in the dynamic stability region. It can also be seen that the dissolution of small crystals (at $r < r_f$) quickly reaches a stationary profile at a given crystallizer operating mode (with constant inflow of substance) (all curves shown in Figure 3 practically coincide at $0 < r < r_f$). The bell-shaped curves shown in Figure 3 at $r > r_f$ are blurred with time due to the growth and withdrawal of crystals from the system at $r = r_p$. Eventually, a bell-shaped form disappears and the non-stationary distribution merges with the stationary one (solid line in Figure 3).

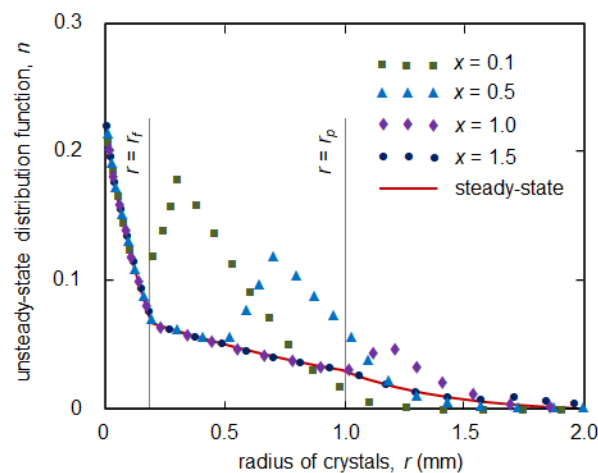


Figure 3. The unsteady-state particle-radius distribution at different decision variables x (symbols) and the steady-state distribution function (solid line). System parameters correspond to Figure 2 with $b = g = 1$. The initial distribution function n_0 was chosen as a normal (Gaussian) distribution with a standard deviation of 0.4 and zero mean.

Let us especially underline characteristic crystallization size and time scales of the theory under consideration. Starting from heterogeneous nucleation in supersaturated solutions, they can be estimated as follows: (i) size of critical nuclei is in the order of 1–10 μm [6], (ii) typical induction times from which primary nucleation kinetics can be established are greater than 10 s [48], (iii) typical sizes of crystals are in the order of 10^{-4} – 10^{-3} m [22], (iv) the typical crystal growth time is greater than 10 s [48], (v) the characteristic length scale of a crystallizer is greater than 0.1 m [22] and (vi) the typical macroscopic time of crystallization is greater than 1000 s [22].

3. Conclusions

In this paper, a theory of continuous operation mode of a crystallizer was developed with allowances for (i) ideal mixing, (ii) isothermal conditions, (iii) constant volumes of solid and liquid phases, (iv) negligible size of nucleating crystals, (v) size-independent growth rate of evolving crystals, (vi) simultaneous crystal nucleation, evolution and fines dissolution, (vii) withdrawal of product crystals and (viii) no crystal fragmentation, attrition, coagulation or Ostwald ripening. The theory was developed on the basis of a population-balance approach. Thus, our theory is based on the nonlinear first-order kinetic equation for the particle-size distribution function and the integro-differential mass balance equation describing the evolution of solute concentration. The exact steady-state solution to this nonlinear model was found analytically, i.e., the steady-state particle-size distribution in various domains of crystal sizes has been derived (Equation (5)). In addition, the steady-state solute concentration is defined by a transcendental equation (Equation (6)). Next, while introducing the logarithm of the distribution function, we rewrote the kinetic equation in integrable form. Using the Laplace transform with respect to the spatial coordinate, this equation was solved analytically. As a result, the unsteady-state particle-size distribution function was found to be dependent on the solute concentration (Equation (12)). To solve this equation together with the integro-differential mass balance equation, we applied the iterative method. Taking small changes in the solute concentration into account, we found the main contributions to the distribution function n_m (Equation (13)) and solute concentration c_m (the Cauchy problem (14) with $n = n_m$). To obtain a more precise distribution function n_1 , we substituted c_m into Equation (12) and arrived at $n_1(r, x)$. Then, by substituting n_1 into the Cauchy problem (14), we came to $c_1(x)$. The iterative procedure can then, in principle, be continued many times. However, our calculations have shown that the first iteration yields a solution that converges on the main approximation.

An important point is that our non-stationary solution tends toward the steady-state solution when time increases. By this we mean that the analytical solution found is stable at a chosen set of parameter values used for calculations. Generally speaking, of course, should we study whether the crystallization process is dynamically stable? To answer this question, one can develop the linear and non-linear dynamic stability theories for the process under consideration. As this takes place, the linear theory only enables us to find a neutral stability surface by dividing the stable and unstable crystallization regions. To calculate the amplitudes of self-oscillatory crystallization, it is necessary to construct a weakly nonlinear stability theory. For this purpose, the cubic terms must be left in the perturbation equations according to the Landau–Hopf nonlinear stability theory. Such a theory can be developed in the near future in the spirit of previous studies of dynamic stability [49–54].

Author Contributions: Conceptualization, E.V.M.; methodology, E.V.M. and D.V.A.; software, E.V.M.; validation, E.V.M. and D.V.A.; formal analysis, E.V.M. and D.V.A.; investigation, E.V.M. and D.V.A.; resources, D.V.A. and A.A.I.; writing—original draft preparation, E.V.M., D.V.A. and A.A.I.; writing—review and editing, E.V.M., D.V.A. and A.A.I.; visualization, E.V.M.; supervision, E.V.M. and D.V.A.; project administration, E.V.M. and D.V.A.; funding acquisition, E.V.M. All authors have read and agreed to the published version of the manuscript.

Funding: This study was supported by the Russian Science Foundation (project number 22-79-00141).

Data Availability Statement: Data are contained within the article.

Conflicts of Interest: The authors declare no conflict of interest.

References

1. Kelton, K.F.; Greer, A.L. *Nucleation in Condensed Matter: Applications in Materials and Biology*; Elsevier: Amsterdam, The Netherlands, 2010.
2. Dubrovskii, V.G. *Nucleation Theory and Growth of Nanostructures*; Springer: Berlin/Heidelberg, Germany, 2014.
3. Vekilov, P.G. Nucleation. *Cryst. Growth Des.* **2010**, *10*, 5007–5019. [[CrossRef](#)] [[PubMed](#)]
4. Rosenberger, F.; Vekilov, P.G.; Muschol, M.; Thomas, B.R. Nucleation and crystallization of globular proteins—What we know and what is missing. *J. Cryst. Growth* **1996**, *168*, 1–27. [[CrossRef](#)]
5. Toropova, L.V.; Makoveeva, E.V.; Osipov, S.I.; Malygin, A.P.; Yang, Y.; Alexandrov, D.V. Nucleation and growth of an ensemble of crystals during the intermediate stage of a phase transition in metastable liquids. *Crystals* **2022**, *12*, 895. [[CrossRef](#)]
6. Mullin, J.W. *Crystallization*; Butterworths: London, UK, 1972.
7. Buyevich, Y.A.; Mansurov, V.V. Kinetics of the intermediate stage of phase transition in batch crystallization. *J. Cryst. Growth* **1990**, *104*, 861–867. [[CrossRef](#)]
8. Alexandrov, D.V.; Nizovtseva, I.G. On the theory of crystal growth in metastable systems with biomedical applications: Protein and insulin crystallization. *Philos. Trans. R. Soc. A* **2019**, *377*, 20180214. [[CrossRef](#)]
9. Buyevich, Y.A.; Goldobin, Y.M.; Yasnikov, G.P. Evolution of a particulate system governed by exchange with its environment. *Int. J. Heat Mass Trans.* **1994**, *37*, 3003–3014. [[CrossRef](#)]
10. Barlow, D.A. Theory of the intermediate stage of crystal growth with applications to protein crystallization. *J. Cryst. Growth* **2009**, *311*, 2480–2483. [[CrossRef](#)]
11. Barlow, D.A. Theory of the intermediate stage of crystal growth with applications to insulin crystallization. *J. Cryst. Growth* **2017**, *470*, 8–14. [[CrossRef](#)]
12. Alexandrov, D.V.; Alexandrova, I.V.; Ivanov, A.A.; Malygin, A.P.; Starodumov, I.O.; Toropova, L.V. On the theory of the nonstationary spherical crystal growth in supercooled melts and supersaturated solutions. *Russ. Metall. (Metally)* **2019**, *2019*, 787–794. [[CrossRef](#)]
13. Alexandrova, I.V.; Ivanov, A.A.; Malygin, A.P.; Alexandrov, D.V.; Nikishina, M.A. Growth of spherical and ellipsoidal crystals in a metastable liquid. *Eur. Phys. J. Spec. Top.* **2022**, *231*, 1089–1100. [[CrossRef](#)]
14. Alexandrova, I.V.; Alexandrov, D.V. Dynamics of particulate assemblages in metastable liquids: A test of theory with nucleation and growth kinetics. *Philos. Trans. R. Soc. A* **2020**, *378*, 20190245. [[CrossRef](#)] [[PubMed](#)]
15. Prieler, R.; Hubert, J.; Li, D.; Verleye, B.; Haberkern, R.; Emmerich, H. An anisotropic phase-field crystal model for heterogeneous nucleation of ellipsoidal colloids. *J. Phys. Condens. Matter* **2009**, *21*, 464110. [[CrossRef](#)] [[PubMed](#)]
16. Kertis, F.; Khurshid, S.; Okman, O.; Kysar, J.W.; Govada, L.; Chayen, N.; Erlebacher, J. Heterogeneous nucleation of protein crystals using nanoporous gold nucleants. *J. Mater. Chem.* **2012**, *22*, 21928–21934. [[CrossRef](#)]
17. Ocaña, M.; Morales, M.P.; Serna, C.J. The growth mechanism of α -Fe₂O₃ ellipsoidal particles in solution. *J. Colloid Int. Sci.* **1995**, *171*, 85–91. [[CrossRef](#)]

18. Shepilov, M.P.; Baik, D.S. Computer simulation of crystallization kinetics for the model with simultaneous nucleation of randomly-oriented ellipsoidal crystals. *J. Non-Crystall. Solids* **1994**, *171*, 141–156. [[CrossRef](#)]
19. Nikishina, M.A.; Alexandrov, D.V. Nucleation and growth dynamics of ellipsoidal crystals in metastable liquids. *Philos. Trans. R. Soc. A* **2021**, *379*, 20200306. [[CrossRef](#)]
20. Nikishina, M.A.; Alexandrov, D.V. Nucleation and growth of ellipsoidal crystals in a supercooled binary melt. *J. Phys. A Math. Theor.* **2022**, *55*, 255701. [[CrossRef](#)]
21. Buyevich, Y.A.; Mansurov, V.V.; Natalukha, I.A. Instability and unsteady processes of the bulk continuous crystallization-I. Linear stability analysis. *Chem. Eng. Sci.* **1991**, *46*, 2573–2578. [[CrossRef](#)]
22. Vollmer, U.; Raisch, J. H_∞ -Control of a continuous crystallizer. *Control Eng. Pract.* **2001**, *9*, 837–845. [[CrossRef](#)]
23. Rachah, A.; Noll, D.; Espitalier, F.; Baillon, F. A mathematical model for continuous crystallization. *Math. Methods Appl. Sci.* **2015**, *39*, 1101–1120. [[CrossRef](#)]
24. Makoveeva, E.V.; Alexandrov, D.V. Mathematical simulation of the crystal nucleation and growth at the intermediate stage of a phase transition. *Russ. Metall. (Metally)* **2018**, *2018*, 707–715. [[CrossRef](#)]
25. Alexandrov, D.V.; Ivanov, A.A.; Nizovtseva, I.G.; Lippmann, S.; Alexandrova, I.V.; Makoveeva, E.V. Evolution of a polydisperse ensemble of spherical particles in a metastable medium with allowance for heat and mass exchange with the environment. *Crystals* **2022**, *12*, 949. [[CrossRef](#)]
26. Janse, A.H. *Nucleation and Crystal Growth in Batch Crystallizers*; Delft University of Technology: Delft, The Netherlands, 1977.
27. Pot, A. *Industrial Sucrose Crystallization*; Delft University of Technology: Delft, The Netherlands, 1980.
28. Kouchi, A.; Tsuchiyama, A.; Sunagawa, I. Effect of stirring on crystallization kinetics of basalt: Texture and element partitioning. *Contr. Mineral. Petrol.* **1986**, *93*, 429–438. [[CrossRef](#)]
29. Adachi, H.; Matsumura, H.; Niino, A.; Takano, K.; Kinoshita, T.; Warizaya, M.; Inoue, T.; Mori, Y.; Sasaki, T. Improving the quality of protein crystals using stirring crystallization. *Jpn. J. Appl. Phys.* **2004**, *43*, L522. [[CrossRef](#)]
30. Alexandrov, D.V. Nucleation and crystal growth kinetics during solidification: The role of crystallite withdrawal rate and external heat and mass sources. *Chem. Eng. Sci.* **2014**, *117*, 156–160. [[CrossRef](#)]
31. Buyevich, Y.A.; Natalukha, I. Unsteady processes of combined polymerization and crystallization in continuous apparatuses. *Chem. Eng. Sci.* **1994**, *49*, 3241–3247. [[CrossRef](#)]
32. Lifshitz, E.M.; Pitaevskii, L.P. *Physical Kinetics*; Pergamon Press: Oxford, UK, 1981.
33. Slezov, V.V. *Kinetics of First-Order Phase Transitions*; Wiley, VCH: Hoboken, NJ, USA, 2009.
34. Alyab'eva, A.V.; Buyevich, Y.A.; Mansurov, V.V. Evolution of a particulate assemblage due to coalescence combined with coagulation. *J. Phys. II Fr.* **1994**, *4*, 951–957. [[CrossRef](#)]
35. Alexandrov, D.V. Kinetics of particle coarsening with allowance for Ostwald ripening and coagulation. *J. Phys. Condens. Matter* **2016**, *28*, 035102. [[CrossRef](#)]
36. Hunt, J.R. Self-similar particle-size distributions during coagulation: Theory and experimental verification. *J. Fluid Mech.* **1982**, *122*, 169–185. [[CrossRef](#)]
37. Alexandrova, I.V.; Alexandrov, D.V.; Makoveeva, E.V. Ostwald ripening in the presence of simultaneous occurrence of various mass transfer mechanisms: An extension of the Lifshitz–Slyozov theory. *Philos. Trans. R. Soc. A* **2021**, *379*, 20200308. [[CrossRef](#)]
38. Alexandrova, I.V.; Alexandrov, D.V. A complete analytical solution of unsteady coagulation equations and transition between the intermediate and concluding stages of a phase transformation. *Eur. Phys. J. Spec. Top.* **2022**, *231*, 1115–1121. [[CrossRef](#)]
39. Toropova, L.V.; Alexandrov, D.V. Dynamical law of the phase interface motion in the presence of crystals nucleation. *Sci. Rep.* **2022**, *12*, 10997. [[CrossRef](#)] [[PubMed](#)]
40. Alexandrov, D.V.; Toropova, L.V. The role of incoming flow on crystallization of undercooled liquids with a two-phase layer. *Sci. Rep.* **2022**, *12*, 17857. [[CrossRef](#)] [[PubMed](#)]
41. Ivanov, A.A.; Alexandrova, I.V.; Alexandrov, D.V. Phase transformations in metastable liquids combined with polymerization. *Philos. Trans. R. Soc. A* **2019**, *377*, 20180215. [[CrossRef](#)] [[PubMed](#)]
42. Buyevich, Y.A.; Mansurov, V.V.; Natalukha, I.A. Instability and unsteady processes of the bulk continuous crystallization-II. Non-linear periodic regimes. *Chem. Eng. Sci.* **1991**, *46*, 2579–2588. [[CrossRef](#)]
43. Natalukha, I.A. Unstable regimes of continuous crystallization in a cascade of well-mixed vessels. *Chem. Eng. Sci.* **1996**, *51*, 1181–1185. [[CrossRef](#)]
44. Ivanov, A.A.; Alexandrova, I.V.; Alexandrov, D.V. Towards the theory of phase transformations in metastable liquids. Analytical solutions and stability analysis. *Eur. Phys. J. Spec. Top.* **2020**, *229*, 365–373. [[CrossRef](#)]
45. Makoveeva, E.V.; Alexandrov, D.V. How the shift in the phase transition temperature influences the evolution of crystals during the intermediate stage of phase transformations. *Eur. Phys. J. Spec. Top.* **2020**, *229*, 2923–2935. [[CrossRef](#)]
46. Ditkin, V.A.; Prudnikov, A.P. *Integral Transforms and Operational Calculus*; Pergamon Press: Oxford, UK, 1965.
47. von Doetsch, G. *Anleitung zum Praktischen Gebrauch der Laplace-Transformation und der Z-Transformation*; R. Oldenbourg: Munich, Germany, 1967.
48. McGinty, J.; Yazdanpanah, N.; Price, C.; ter Horst, J.H.; Sefcik, J. Nucleation and crystal growth in continuous crystallization. In *The Handbook of Continuous Crystallization*; Yazdanpanah, N., Nagy, Z.K., Eds.; Royal Society of Chemistry: London, UK, 2020; pp. 1–50.

49. Alexandrov, D.V. A nonlinear instability analysis of crystallization processes with a two-phase zone. *J. Metast. Nanocrystalline Mater.* **2004**, *20–21*, 468–473. [[CrossRef](#)]
50. Alexandrov, D.V. Absolute morphological stability of the self-similar solidification with a planar front. *J. Metast. Nanocrystalline Mater.* **2004**, *20–21*, 476–481. [[CrossRef](#)]
51. Feltham, D.L.; Worster, M.G. Flow-induced morphological instability of a mushy layer. *J. Fluid Mech.* **1999**, *391*, 337–357. [[CrossRef](#)]
52. Anderson, D.M.; Worster, M.G. A new oscillatory instability in a mushy layer during the solidification of binary alloys. *J. Fluid Mech.* **1996**, *307*, 245–267. [[CrossRef](#)]
53. Alexandrov, D.V.; Malygin, A.P. Flow-induced morphological instability and solidification with the slurry and mushy layers in the presence of convection. *Int. J. Heat Mass Trans.* **2012**, *55*, 3196–3204. [[CrossRef](#)]
54. Alexandrov, D.V.; Ivanov, A.O. Dynamic stability analysis of the solidification of binary melts in the presence of a mushy region: Changeover of instability. *J. Cryst. Growth* **2000**, *210*, 797–810. [[CrossRef](#)]